CAMx Ozone Source Attribution in the Eastern United States using Guidance from Observations during DISCOVER-AQ Maryland

Daniel L. Goldberg[a,*], Timothy P. Vinciguerra[b], Daniel C. Anderson[a], Linda Hembeck[a], Timothy P. Canty[a], Sheryl H. Ehrman[b], Douglas K. Martins[c], Ryan M. Stauffer[c,d], Anne M. Thompson[c,e], Ross J. Salawitch[a,d,f], and Russell R. Dickerson[a,d,f]

[a]Department of Atmospheric and Oceanic Science, University of Maryland, College Park, MD 20742, USA

[b]Department of Chemical and Biomolecular Engineering, University of Maryland, College Park, MD 20742, USA

[c]Department of Meteorology, Penn State University, University Park, PA 16802, USA

[d]Earth System Science Interdisciplinary Center, University of Maryland, College Park, MD 20740, USA

[e]NASA Goddard Space Flight Center, Code 614, Greenbelt, MD 20771, USA

[f]Department of Chemistry, University of Maryland, College Park, MD 20742, USA

*Corresponding author. Tel.: +1 860 424 6851.

E-mail address: dgoldb@atmos.umd.edu (D. L. Goldberg)

Submitted to *Geophysical Research Letters* on December 7, 2015

Revised on February 5, 2016

Key points

- Ozone is simulated well by CAMx, but there is an overestimate of NO_y and underestimate of HCHO.
- Ozone production in the new model framework is more sensitive to NO_x emissions.
- Point sources likely contribute more to surface ozone than commonly appreciated.

Abstract

A Comprehensive Air-Quality Model with Extensions (CAMx) version 6.10 simulation was assessed through comparison with data acquired during NASA's 2011 DISCOVER-AQ Maryland field campaign. Comparisons for the baseline simulation (CB05 chemistry, EPA 2011 National Emissions Inventory) show a model overestimate of NO_y by +86.2% and an underestimate of HCHO by –28.3%. We present a new model framework (CB6r2 chemistry, MEGAN v2.1 biogenic emissions, 50% reduction in mobile NO_x, enhanced representation of isoprene nitrates) that better matches observations. The new model framework attributes 31.4% more surface ozone in Maryland to electric generating units (EGUs) and 34.6% less ozone to on-road mobile sources. Surface ozone becomes more NO_x-limited throughout the eastern United States compared to the baseline simulation. The baseline model therefore likely underestimates the effectiveness of anthropogenic NO_x reductions as well as the current contribution of EGUs to surface ozone.

1. Introduction

Policymakers and regulatory agencies use regional air quality models to predict how future air quality will respond to control strategies [EPA, 2014a]. Many air quality models can skillfully simulate surface ozone in North America for focused studies of certain time periods [Hogrefe et al., 2004; Appel et al., 2007; Ferreira et al., 2011; Appel et al., 2012; Simon et al., 2012]. Global models can reflect changes in ozone resulting from control measures [e.g., Clifton et al., 2014; Rieder et al., 2015], especially for rural sites representative of regional atmospheric composition, but nonattainment is based on monitors with the highest readings. Urban-scale events, such as seen in Edgewood, MD, discussed below, require urban scale resolution of 12 km or better [e.g., Loughner et al., 2011; Goldberg et al., 2014].

Even where regional air quality models accurately reproduce surface ozone concentrations, many have difficulty simulating the response of ozone to reductions in precursor emissions [Gilliland et al., 2008; Zhou et al., 2013; Foley et al., 2015]. This may be linked to the challenge of simulating ozone precursors: NO_x ($NO_x = NO+NO_2$) and volatile organic compounds (VOCs) [Castellanos et al., 2011; Zhou et al., 2013; Canty et al., 2015]. For any given ozone concentration, there can be many different production pathways; empirical kinetic modeling approach (EKMA) diagrams [Kinosian, 1982; Chameides et al., 1992; Sillman, 1999], highlight this non-linear dependence of ozone production on NO_x and VOCs. Air quality models must be in the correct ozone production regime (i.e., NO_x-limited vs. VOC-limited) if they are to accurately forecast how air quality regulations will improve ozone concentrations.

Many studies show an overestimate, by up to a factor of two, of total reactive oxidized nitrogen (NO_y) in regional air quality models compared to observations [Doraiswamy et al., 2009; Castellanos et al., 2011; Yu et al., 2012; Brioude et al., 2013; Anderson et al., 2014; Goldberg et al., 2014]. Some link the calculation of too much NO_y to the overestimate of NO_x emissions from area sources [Doraiswamy et al., 2009], while others link it to an overestimate of NO_x emissions from commercial marine vessels [Brioude et al., 2013]. Anderson et al. [2014] examined airborne observations of CO, NO_x, and NO_y obtained in the Baltimore-Washington corridor and concluded that a substantial portion of the error must be due to an overestimate in NO_x emissions from mobile sources since this source accounts for the majority (62%) of NO_x emissions in the 2011 National Emissions Inventory (NEI). Fujita et al. [2012] also find an overestimate of NO_x mobile source emissions in MOVES 2010a, which is used to develop the NEI.

A better representation of NO_y chemistry may resolve a portion of the overestimate of NO_y noted above. The Carbon Bond 6 Revision 2 (CB6r2) gas-phase chemistry has been released recently [Hildebrandt-Ruiz and Yarwood, 2013]. This updated mechanism more explicitly represents alkyl nitrates in regional air quality models and provides a

significant improvement in the simulation of these compounds compared to CB05 [Hildebrandt-Ruiz and Yarwood, 2013; Canty et al., 2015]. CB6r2 splits the alkyl nitrate grouping (NTR) into three families: alkyl nitrates that exist primarily in the gas phase (NTR1), larger multi-functional alkyl nitrates that partition to organic aerosol (NTR2) and isoprene nitrates (INTR) that react rapidly with OH. NTR1 and INTR can recycle back to NO_2, but the only gas-phase sink for NTR2 is conversion to HNO_3. The CB6r2 gas-phase mechanism calculates a shorter lifetime of alkyl nitrates and faster recycling of NO_x, which agrees better with laboratory studies [Perring et al., 2013] than CB05. In addition to improving the representation of alkyl nitrates in the regional air quality models, this change may also improve the simulation of ozone attributed to sources beyond state borders. To further improve the representation of alkyl nitrates in air quality models, Horowitz et al. [2007] suggest increasing isoprene nitrate deposition velocities.

As anthropogenic sources of ozone precursors continue to decrease, biogenic emissions will play an even larger role in the ozone formation process. Two models are used to simulate biogenic emissions within regional air quality models: Biogenic Emissions Inventory System (BEIS) [Pouliot and Pierce, 2009] and Model of Emissions of Gases and Aerosols from Nature (MEGAN) [Guenther et al., 2012]. Isoprene emissions are uniformly larger in the MEGAN model within North America than in BEIS [Warneke et al., 2010; Carlton and Baker 2011].

2. Methods

We use the Comprehensive Air-quality Model with Extensions (CAMx) version 6.10 to simulate trace gas mixing ratios in the eastern United States for July 2011; the model domain is shown in Figure S1. Many previous studies have used CAMx to simulate ozone with reasonable fidelity [Emery et al., 2012; Dolwick et al., 2015; Koo et al., 2015]. The Anthropogenic Precursor Culpability Assessment (APCA) probing tool in CAMx is used as a means to tag ozone source attribution from twelve source regions and seven source sectors. The twelve source regions are shown in Figure S2. The seven source sectors are listed in Table S1. We also use the Ozone Source Apportionment Tool (OSAT) to calculate the ozone attributed to NO_x- and VOC-limited production regimes. For a detailed description of CAMx v6.10 and the APCA and OSAT probing tools, please refer to the CAMx User's Guide [Ramboll Environ, 2014]. CAMx was driven off-line by meteorological output [EPA, 2014b] from the WRF v3.4 model [Skamarock et al., 2008] at hourly intervals. Specific details about the meteorology simulation are in the EPA technical support document [EPA, 2014b]. Table S2 describes the CAMx options chosen for our baseline simulation.

We use version 2 of the 2011 NEI as compiled by EPA for anthropogenic emissions in our baseline simulation [EPA, 2014c]. The Continuous Emission Monitoring System (CEMS) database temporalized by Eastern Regional Technical Advisory Committee

(ERTAC) software was used to create electric generation unit (EGU) emissions. This inventory allocates larger emissions of NO_x during hotter days due to increased electricity demand [He et al., 2013], but does not include an estimate of additional NO_x emitted by small peaking units. Mobile emissions estimates from cars, trucks, and motorcycles were computed with the Motor Vehicle Emission Simulator 2014 (MOVES2014) [EPA, 2014c]. Biogenic emissions in the baseline simulation were calculated using BEIS version 3.6 [Pouliot and Pierce, 2009]. The Mid-Atlantic Regional Air Management Association (MARAMA) prepared total emissions for our model domain. Boundary conditions were initialized using the GEOS-Chem v8-03-02 global chemistry model [Bey et al., 2001] at a horizontal resolution of 2.0° latitude × 2.5° longitude, as described in Henderson et al. [2014].

3. Results

3.1 Baseline Model Simulation

During July 2011, NASA conducted a comprehensive aircraft and ground measurement campaign in Maryland called DISCOVER-AQ. This campaign provided a temporally- and spatially-rich collection of trace gas and aerosol observations throughout the lower troposphere [Crawford et al., 2014]. This dataset offers an unprecedented opportunity to compare regional air quality models to comprehensive atmospheric observations.

Figure 1 (left) compares ozone (O_3) and two important ozone precursors, NO_y and formaldehyde (HCHO), from the baseline model simulation to P3-B aircraft observations. All observations were taken between altitudes of 300 – 5000 m within the Maryland airshed. In the top left – the scatterplot of modeled ozone vs. observed ozone – we show a slope near unity (1.06) and a normalized mean bias (NMB) of –6.90% indicating a small underestimate of ozone above the surface. Because the NMB is under 10%, the baseline simulation shows good agreement with the observations of ozone. The root-mean square error (RMSE) of the baseline simulation of ozone is 9.88 ppbv. In the supplementary material, Figure S3, we provide a comparison to surface observations, which shows even better agreement with the baseline simulation.

Comparing modeled NO_y and HCHO to observations of the same quantities shows large discrepancies. The model simulation overestimates NO_y by nearly a factor of two: a slope of 1.91 and a NMB of +86.2%. An overestimate of NO_y is also seen at the Edgewood, Maryland ground site as shown in Figure S4; instrument description is provided in Martins et al. [2012]. Conversely, the model simulation underestimates HCHO by nearly a factor of two: a slope of 0.61 and a NMB of –28.3%. Although ozone is being predicted with considerable skill, the ozone precursors (NO_y and HCHO) are not. In the supplementary material, Figures S5, S6, S7 and S8, we show comparisons of NO_2, alkyl nitrates, nitric acid, and isoprene.

The overestimate of NO_y and underestimate of HCHO by the baseline model simulation are more pronounced at the lowest altitudes of the P3-B aircraft spirals. In Figure 2, we show vertical profiles of measured ozone, NO_y, and HCHO binned in 500 m intervals and the closest CAMx model grid point, matched spatially and temporally during all flights. The median value of observed NO_y at the lowest altitude is below the 25th percentile of simulated NO_y, while the median value of observed HCHO is above the 75th percentile of simulated HCHO. We also find that ozone is underestimated for the lowest sampled altitudes, but agrees well with observations above 2.5 km; the underestimate of ozone, however, is not seen directly at the surface (Figure S3).

3.2 Updated "Beta" Model Simulation

We update the CAMx model platform based on recommendations from recent scientific literature outlined in the Introduction. The four changes are:

- Update the gas-phase chemistry from CB05 to CB6r2, which better represents alkyl nitrate photochemistry [Hildebrandt-Ruiz and Yarwood, 2013].
- Update the biogenic emissions from BEIS v3.6 to MEGAN v2.1, which increases isoprene emissions [Guenther et al., 2012].
- Reduce NO_x emissions from mobile sources (on-road, off-road and non-road) by 50% within our model domain [Anderson et al., 2014].
- Increase the dry deposition velocities of isoprene nitrates (INTR) and multi-functional alkyl nitrates (NTR2) to be the same as nitric acid (HNO_3) [Horowitz et al., 2007].

We label the CAMx simulation with these four changes as the "Beta" simulation and compare the same trace gases (O_3, NO_y, HCHO) from this updated run to P3-B aircraft observations in the right side of Figure 1. The Beta simulation exhibits substantial improvement in the estimate of ozone precursors. The NMB of NO_y has improved from +86.2% to +22.4% and the NMB of HCHO has improved from –28.3% to –0.47%. The RMSE of NO_y and HCHO both improve: NO_y from 3.09 ppbv to 1.71 ppbv and HCHO from 1.34 ppbv to 0.93 ppbv. The NMB of NO_y at the Edgewood, MD ground monitor also improves from +46.9% to –7.8% using this new model platform (Figure S4). The Beta simulation yields similar predictions of ozone compared to the original calculation: the baseline has a NMB of –6.90%, whereas the Beta simulation has a NMB of –7.82%. The RMSE of the ozone degrades slightly from 9.88 ppbv to 10.53 ppbv. Deteriorating performance of ozone in the Beta simulation may be due to not enough recycling of multi-functional alkyl nitrates to NO_2 in the CB6r2 gas-phase mechanism.

The Beta simulation also shows better agreement with the vertical profiles of NO_y and HCHO (Figure 2). The median value of observed NO_y is much closer to the median

196 value of modeled NO_y. At altitudes above 2.5 km, there is no improvement in the
197 simulation of NO_y, likely due to an overestimate of HNO_3 within the GEOS-Chem global
198 model used to initialize the CAMx boundaries (Figure S9). At these altitudes, HNO_3 is
199 photochemically inactive and the overestimate will have minimal impact on ozone
200 formation. The median value of observed HCHO is also much closer to the median value
201 of HCHO from the Beta simulation. However, there is now a large overestimate in the
202 simulation of isoprene (Figure S6), which suggests errors in the isoprene to formaldehyde
203 conversion processes in CB6r2. Mao et al. [2013] show that improvements to isoprene
204 oxidation processes in air quality models are still needed. We also compare the isoprene
205 observations to a CAMx simulation with a recently released version of BEIS v3.61 [Bash
206 et al., 2015], which shows the best agreement with observations (Figure S10); BEIS
207 v3.61 has improved land-use and canopy representation. Similar to our study, Kota et al.
208 [2015] also showed an overestimate of isoprene using MEGAN v2.1 in southeast Texas.
209 The comparison of observed ozone to values from the Beta simulation exhibits similar
210 features as the comparison for the baseline simulation. The NMB of seven trace gases for
211 the baseline, each modification isolated separately, and Beta simulations are given in
212 Table S3.

213 **3.3 Changes to Ozone Attributed to Mobile vs. Large Point Sources**

214 The NEI shows on-road and off-road mobile source emissions account for the largest
215 portion of the total NO_x emissions, 61% of the total (Figure S11). In Maryland the
216 percentage is even larger; NO_x emissions from on-road and off-road sources account for
217 72% of total NO_x emissions. Figure 3 depicts ozone attributed to emissions from
218 individual states (denoted by color) as well as from various source sectors (each
219 histogram). Results are shown for both the (left) baseline and (right) Beta simulations,
220 for the ten worst modeled air quality days in July 2011 at Edgewood, Maryland; observed
221 surface ozone during these ten days is 81.3 ppbv (only six of the top ten worst modeled
222 days match the top ten worst observed days). We have chosen to focus on Edgewood
223 (the location shown as the filled circle in Figure 4) because this site causes the Baltimore
224 region to be in moderate non-attainment of the 2008 NAAQS for ozone [EPA, 2014a]. In
225 the baseline simulation (Figure 3, left) – generated from the NEI – on-road sources are
226 responsible for the largest portion (24.6 ppbv) of total surface ozone. Ozone attributed to
227 electric generating units (EGUs) accounts for the second largest single sector (11.6 ppbv)
228 during the ten worst air quality days at Edgewood. The NEI indicates EGUs are
229 responsible for 14% of total NO_x emissions, and 11% within the state of Maryland.

230 In the Beta simulation we keep emissions from EGUs identical to the baseline simulation
231 because the NEI is developed from observed Continuous Emissions Monitoring System
232 (CEMS) data. There is strong scientific basis [Anderson et al., 2014] to link the
233 overestimate in NO_y to mobile source emissions since they represent more than 50% of
234 the NO_x emissions inventory. The Beta simulation (Figure 3, right) attributes more ozone

to EGUs and less ozone to mobile sources. While on-road mobile sources are still the primary individual source sector contributing to surface ozone, they are responsible for 7.7 ppbv less ozone compared to the baseline simulation: 24.6 ppbv to 16.9 ppbv, a drop of 31.4%. Ozone attributed to non-road sources also shows a similar percentage drop. Despite identical emissions of NO_x from EGUs in the two simulations, electricity generation is responsible for 4.0 ppbv more ozone in the Beta run, increasing from 11.6 to 15.6 ppbv, a 34.6% increase. The ozone attributed to EGU emissions shows a large increase because CB6r2 gas-phase chemistry has faster photolysis of NO_2 than CB05 and increased modeled HO_2 and RO_2 concentrations driven by greater biogenic emissions from MEGAN v2.1. This implies greater ozone production efficiency, a topic to be treated in a separate paper. For the Beta simulation, EGUs and on-road mobile sources are now responsible for roughly the same fraction of surface ozone in Maryland. The change in surface ozone attribution to on-road mobile and EGU sources for the baseline compared to the Beta simulation is similar throughout the eastern United States for July 2011 (Figure S12).

3.4 Changes to Ozone Attributed to NO_x & VOC limitations

The overestimate of NO_y and underestimate of HCHO in the baseline simulation suggests that ozone in the original model framework may be produced in a more VOC-limited ozone production regime than occurs in the actual atmosphere, even though NO_x remains the key pollutant. To better grasp the relationship between modeled and observed ozone precursors, we plot ozone as a function of NO_y for the observations and two model simulations (Figure S13). The observed slope of the linear-best fit indicates 20.9 ppbv of ozone per ppbv of NO_y in the Maryland airshed, whereas, the baseline simulation indicates a slope of 8.6. Ozone becomes more sensitive to NO_y in the updated Beta model platform, which yields a slope of 13.3. We also compare HCHO as a function of NO_y (Figure S14). The linear best fit of the observations show 1.39 ppbv of HCHO per ppbv of NO_y; the baseline model has a linear fit of 0.45, but the Beta simulation show a slope of 1.28, which is closer to the observations. The sensitivity of ozone to the abundance of its precursors is captured better in the updated Beta model platform.

We also use an OSAT simulation to calculate the amount of ozone formed in NO_x-limited and VOC-limited environmental conditions. Figure 4 shows the percentage of ozone production attributed to a NO_x-limited ozone regime. In the baseline simulation, 65 – 85% of ozone in the Baltimore vicinity is attributed to a NO_x-limited environment. The updated Beta simulation uniformly shows more ozone production in a NO_x-limited regime. The biggest differences occur over the Chesapeake Bay. The Beta simulation shows 80 – 95% of ozone is produced in a NO_x-limited environment in the Baltimore vicinity. Instead of being in the "transition region" – the region on the EKMA diagram in which ozone production occurs due to both VOC and NO_x limitation – the area is now

squarely in a region of NO_x-limited ozone production. This is consistent with observed changes in ozone resulting from NO_x emission reductions [Gilliland et al., 2008].

3.5 Changes to Ozone Source Region Attribution

Modifications to the model framework do not have a big effect on source attribution, but subtle differences are worth discussing. Figure S15 shows state-by state attribution at the Edgewood, Maryland monitor for the ten worst modeled air quality days during July 2011 for the baseline and Beta simulations. Maryland is the largest contributor to total ozone mixing ratios at Edgewood. States upwind of Maryland during hot summertime days, i.e. Pennsylvania, Virginia, and Ohio contribute more than 4 ppbv each. Further discussion on the interstate transport of ozone is included in Goldberg et al. [2015]. When changing model platforms, Maryland shows a slight rise in attribution (27.9 ppbv to 29.1 ppbv), while other states show small declines in ozone attribution (i.e., Virginia). The changes do not shift any state from being above or below 1 ppbv – a critical value legislated by the Cross-State Air Pollution Rule (CSAPR).

Each individual incremental change to the modeling platform alters the source region attribution. Figure S16 shows source region attribution of surface ozone at Edgewood during the ten worst air quality days in July for five simulations in three scenarios: baseline, baseline with CB6r2 and increased alkyl nitrate depoistion, baseline with MEGAN v2.1 biogenics, baseline with 50% mobile NO_x emissions, and Beta. For the baseline simulation (left), Maryland is responsible for 30.9% of the total; interstate transport accounts for the other 69.1%. Improvement of the alkyl nitrate photochemistry and the mobile emissions inventory make ozone photochemistry more of a regional problem, as shown by the slightly reduced contributions from Maryland in the CB6r2+NTRdepn and 50% mobile NOx simulations, 29.3% and 30.0% respectively. Changes to the biogenic emissions inventory, resulting in increased isoprene, make ozone photochemistry more of a local issue, with Maryland's contribution in the MEGAN v2.1 increasing to 36.0%.

4. Conclusion

CAMx, when modified with guidance provided by a field experiment, more realistically simulates the observed abundance of ozone precursors. We compare ozone precursors (NO_y and HCHO) and ozone measured during the July 2011 DISCOVER-AQ Maryland campaign to CAMx simulations. In the baseline simulation, there is good agreement between modeled and observed ozone, but poor agreement for NO_y and HCHO. We implemented four changes to the model: CB6r2 gas-phase chemistry, faster deposition of alkyl nitrates, reduced NO_x emissions from mobile sources, and increased isoprene emissions by switching to MEGAN v2.1 biogenic emissions. Our results indicate that BEIS v3.61 shows good agreement with isoprene observations, and we recommend this

over BEIS v3.6. The Beta runs dramatically improve the simulation of total reactive nitrogen, alkyl nitrates, and formaldehyde. Adding more recycling of alkyl nitrates to NO_2 in CB6r2 and refining isoprene photochemistry may further improve CAMx performance.

These modifications change the attribution of ozone to different source sectors and have important policy implications. Compared to the baseline simulations, mobile sources contribute 31.4% less to total ozone while EGUs contribute 34.6% more at Edgewood, Maryland. Ozone attributed to EGUs increase from 11.6 to 15.6 ppbv, while ozone attributed to mobile sources decreases from 24.6 to 16.9 ppbv. Ozone in the two model simulations is comparable and agrees reasonably well with observations, but the source attribution and targets for control strategies change substantially.

Prior research demonstrated that regional air quality models underestimate the benefit of NO_x control measures for surface ozone. If air quality models are used to forecast how future air quality regulations will affect surface ozone, they must simulate ozone within the correct production regime (i.e., NO_x-limited vs. VOC-limited). For the Baltimore area, this updated model platform increases the percentage of the ozone formed in a NO_x-limited regime from ~75 to ~85% of the total. Since the updated model platform places ozone in a more NO_x-limited regime, it is possible a simulation of surface ozone long-term trends using these changes will resolve the long-standing difficulty in simulating the response of surface ozone to past reductions in ozone precursors.

Acknowledgments

We would like to thank Andrew Weinheimer, Alan Fried, Ron Cohen, and Armin Wisthaler for their observations of trace gases from the P3-B aircraft during DISCOVER-AQ Maryland. All data from DISCOVER-AQ Maryland can be downloaded freely from http://www-air.larc.nasa.gov/cgi-bin/ArcView/discover-aq.dc-2011. We would also like to thank Julie McDill and Susan Wierman from MARAMA for preparation of the emissions. The Maryland Department of the Environment (MDE) (G. Tad Aburn, Michael Woodman, and Jennifer Hains), the NASA Air Quality Applied Sciences Team (AQAST), and the NASA Modeling, Analysis, and Prediction (MAP) program all funded this research. CAMx source code has been provided by Ramboll Environ and can be freely downloaded from http://www.camx.com.

Bibliography

Anderson, D. C., C. P. Loughner, G. Diskin, A. Weinheimer, T. P. Canty, R. J. Salawitch, H. M. Worden, A. Fried, T. Mikoviny, A. Wisthaler, and R. R. Dickerson (2014), Measured and modeled CO and NOy in DISCOVER-AQ: An evaluation of emissions and chemistry over the eastern US. *Atmos. Environ.,* 96, 78-87.

Appel, K. W., A. B. Gilliland, G. Sarwar, and R. C. Gilliam (2007), Evaluation of the Community Multiscale Air Quality (CMAQ) model version 4.5: Sensitivities impacting model performance Part I - Ozone. *Atmos. Environ.*, *41*(40), 9603-9615. doi:10.1016/j.atmosenv.2007.08.044

Appel, K. W., C. Chemel, S. J. Roselle, X. V. Francis, R. Hu, R. S. Sokhi, S.T. Rao, and S. Galmarini (2012), Examination of the Community Multiscale Air Quality (CMAQ) model performance over the North American and European domains. *Atmos. Environ.,* 53, 142-155.

Bash, J.O., K.R. Baker, and M.R. Beaver (2015), Evaluation of improved land use and canopy representation in BEIS v3.61 with biogenic VOC measurements in California. *Geosci. Model Dev. Disc., 8*, 8117–8154.

Bey, I., D. J. Jacob, R. M. Yantosca, J. A. Logan, B. D. Field, A. M. Fiore, Q. B. Li, H. G. Y. Liu, L. J. Mickley, and M. G. Schultz (2001), Global modeling of tropospheric chemistry with assimilated meteorology: Model description and evaluation. *J. Geophys. Res.-Atmos.*, *106*(D19), 23073-23095.

Brioude, J., W. M. Angevine, R. Ahmadov, S.-W. Kim, S. Evan, S. A. McKeen, E.-Y. Hsie, G. J. Frost, J. A. Neuman, I. B. Pollack, J. Peischl, T. B. Ryerson, J. Holloway, S. S. Brown, J. B. Nowak, J. M. Roberts, S. C. Wofsy, G. W. Santoni, T. Oda, and M. Trainer (2013), Top-down estimate of surface flux in the Los Angeles Basin using a mesoscale inverse modeling technique: assessing anthropogenic emissions of CO, NO_x, and CO2 and their impacts. *Atmos. Chem. Phys.,* 13, 3661-3677.

Canty, T. P., L. Hembeck, T. P. Vinciguerra, D. C. Anderson, D. L. Goldberg, S. F. Carpenter, D. J. Allen, C. P. Loughner, R. J. Salawitch, and R. R. Dickerson (2015), Ozone and NO x chemistry in the eastern US: evaluation of CMAQ/CB05 with satellite (OMI) data. *Atmos. Chem. Phys.*, *15*, 10965-10982.

Carlton, A. G, and K. R. Baker (2011), Photochemical Modeling of the Ozark Isoprene Volcano: MEGAN, BEIS, and Their Impacts on Air Quality Predictions. *Environ. Sci. Technol.,* 45, 4438-4445.

Castellanos, P., L. T. Marufu, B. G. Doddridge, B. F. Taubman, J. J. Schwab, J. C. Hains, S. H. Ehrman, and R. R. Dickerson (2011), Ozone, oxides of nitrogen, and carbon monoxide during pollution events over the eastern United States: An evaluation of emissions and vertical mixing. *J. Geophys. Res.-Atmos.*, *116*, D16307. doi:10.1029/2010JD014540

Chameides, W. L., F. Fehsenfeld, M. O. Rodgers, C. Cardelino, J. Martinez, D. Parrish, W. Lonneman, D. R. Lawson, R. A. Rasmussen, P. Zimmerman, J. Greenberg, P. Middleton, and T. Wang (1992), Ozone precursor relationships in the ambient atmosphere. *Journal of Geophys. Res.-Atmos., 97*(D5), 6037-6055

Crawford, J. H., R. R. Dickerson, and J. Hains (2014), DISCOVER-AQ Observations and early results. *Environmental Manager*, 8-15.

385 Dolwick, P., F. Akhtar, K. R. Baker, N. Possiel, H. Simon, and G. Tonnesen (2015)
386 Comparison of background ozone estimates over the western United States based on
387 two separate model methodologies. *Atmos. Environ., 109*, 282–296.
388 Doraiswamy, P., C. Hogrefe, W. Hao, R. F. Henry, K. Civerolo, J. Ku, G. Sistla, J. J.
389 Schwab, and K. L. Demerjian (2009), A diagnostic comparison of measured and
390 model-predicted speciated VOC concentrations. *Atmos. Environ., 43*, 5759-5770.
391 Emery, C., J. Jung, N. Downey, J. Johnson, M. Jimenez, G. Yarwood, and R. Morris
392 (2012), Regional and global modeling estimates of policy relevant background ozone
393 over the United States. *Atmos. Environ., 47*, 206–217.
394 Emmons, L. K., S. Walters, P. G. Hess, J.-F. Lamarque, G. G. Pfister, D. Fillmore, C.
395 Granier, A. Guenther, D. Kinnison, and T. Laepple (2010), Description and evaluation
396 of the Model for Ozone and Related chemical Tracers, version 4 (MOZART-4). *Geosci.*
397 *Model Dev.*, *3*(1), 43-67.
398 EPA. (2014a). Modeling Guidance for Demonstrating Attainment of Air Quality Goals
399 for Ozone, PM2.5, and Regional Haze. Retrieved November 2015 from
400 http://www.epa.gov/ttn/scram/guidance/guide/Draft_O3-PM-RH_Modeling_Guidance-
401 2014.pdf
402 EPA. (2014b). Meteorology Technical Support Document - Meteorological Model
403 Performance for Annual 2011 WRF v3.4 Simulation. Retrieved November 2015 from
404 http://www.epa.gov/ttn/scram/reports/MET_TSD_2011_final_11-26-14.pdf
405 EPA. (2014c). Technical Support Document (TSD) Preparation of Emissions Inventories
406 for the Version 6.2, 2011 Emissions Modeling Platform. Retrieved November 2015
407 from
408 http://www3.epa.gov/ttn/chief/emch/2011v6/2011v6_2_2017_2025_EmisMod_TSD_a
409 ug2015.pdf
410 EPA. (2014d). Air Quality Designations for the 2008 Ozone National Ambient Air
411 Quality Standards. Retrieved November 2015 from
412 http://www.epa.gov/oaqps001/greenbk/hindex.html
413 Fehsenfeld, F. C., R. R. Dickerson, G. Hubler, W. T. Luke, L. J. Nunnermacker, E. J.
414 Williams, J. M. Roberts, J. G. Calvert, C. M. Curran, and A. C. Delany (1987), A
415 ground-based intercomparison of NO, NOx, and NOy measurement techniques.
416 *Journal of Geophys. Res.-Atmos., 92*(12), 710–722.
417 Ferreira, J., A. Rodriguez, A. Monteiro, A. Miranda I, M. Dios, J. A. Souto, G. Yarwood,
418 U. Nopmongcol, and C. Borrego (2011), Air quality simulations for North America-
419 MM5-CAMx modelling performance for main gaseous pollutants. *Atmos. Environ., 52,*
420 212-224
421 Fiore, A. M., J. T. Oberman, M. Y. Lin, L. Zhang, O. E. Clifton, D. J. Jacob, V. Naik, L.
422 W. Horowitz, J. P. Pinto, and G. P. Milly (2014), Estimating North American
423 background ozone in U.S. surface air with two independent global models: Variability,
424 uncertainties, and recommendations. *Atmos. Environ.*, *96*, 284-300.
425 doi:10.1016/j.atmosenv.2014.07.045
426 Foley, K. M, C. Hogrefe, G. Pouliot, N. Possiel, S. J. Roselle, H. Simon, and B. Timin
427 (2015), Dynamic evaluation of CMAQ part I: Separating the effects of changing
428 emissions and changing meteorology on ozone levels between 2002 and 2005 in the
429 eastern US. *Atmos. Environ., 103*, 247-255.

Fujita, E. M., D. E. Campbell, B. Zielinska, J. C. Chow, C. E. Lindhjem, A. DenBleyker, G. A. Bishop, B. G. Schuchmann, D. H. Stedman, and D. R. Lawson (2012), Comparison of the MOVES2010a, MOBILE6.2, and EMFAC2007 mobile source emission models with on-road traffic tunnel and remote sensing measurements. *Journal of the Air & Waste Management Association* 62, no. 10: 1134-1149.

Gilliland, A. B., C. Hogrefe, R. W. Pinder, J. M. Godowitch, K. L. Foley, and S. T. Rao (2008), Dynamic evaluation of regional air quality models: assessing changes in O 3 stemming from changes in emissions and meteorology. *Atmos. Environ.*, *42*, 5110-5123.

Goldberg, D. L., T. P. Vinciguerra, K. M. Hosley, C. P. Loughner, T. P. Canty, R. J. Salawitch, and R. R. Dickerson (2015), Evidence for an increase in the ozone photochemical lifetime in the eastern United States using a regional air quality model. *Journal of Geophys. Res.-Atmos., 120*, 12,778–12,793.

Goldberg, D. L., C. P. Loughner, M. Tzortziou, J. W. Stehr, K. E. Pickering L. T. Marufu, and R. R. Dickerson (2014), Higher surface ozone concentrations over the Chesapeake Bay than over the adjacent land: Observations and models from the DISCOVER-AQ and CBODAQ campaigns. *Atmos. Environ.*, *84*, 9-19.

Guenther, A. B., X. Jiang, C. L. Heald, T. Sakulyanontvittaya, T. Duhl, L. K. Emmons, and X. Wang (2012), The Model of Emissions of Gases and Aerosols from Nature version 2.1 (MEGAN2.1): an extended and updated framework for modeling biogenic emissions. *Geosci. Model Dev.*, *5*(6), 1471-1492. doi:10.5194/gmd-5-1471-2012

He, H., J. W. Stehr, J. C. Hains, D. J. Krask, B. G. Doddridge, K. Y. Vinnikov, T. P. Canty, K. M. Hosley, R. J. Salawitch, and R. R. Dickerson (2013), Trends in emissions and concentrations of air pollutants in the lower troposphere in the Baltimore/Washington airshed from 1997 to 2011. *Atmos. Chem. Phys.*, 13, 1-16.

Henderson, B. H., F. Akhtar, H. O. T. Pye, S. L. Napelenok, and W. T. Hutzell (2014), A database and tool for boundary conditions for regional air quality modeling: description and evaluation. *Geosci. Model Dev.*, *7*(1), 339-360.

Hildebrandt-Ruiz, L., and G. Yarwood (2013), Interactions between Organic Aerosol and NOy: Influence on Oxidant Production. Final report for AQRP project 12-012. Prepared for the Texas Air Quality Research Program.

Hogrefe, C., J. Biswas, B. Lynn, K. Civerolo, J. Y. Ku, J. Rosenthal, C. Rosenzweig, R. Goldberg, and P. L. Kinney (2004), Simulating regional-scale ozone climatology over the eastern United States: model evaluation results. *Atmos. Environ.,* 38, 2627-2638.

Horowitz, L. W., A. M. Fiore, G. P. Milly, R. C. Cohen, A. Perring, P. J. Wooldridge, P. G. Hess, L. K. Emmons, and J. F. Lamarque (2007), Observational constraints on the chemistry of isoprene nitrates over the eastern United States. *J Geophys Res-Atmos*, *112*, D12S08. doi:10.1029/2006JD007747

Houyoux, M. R., and J. M. Vukovich (1999), Updates to the Sparse Matrix Operator Kernel Emissions (SMOKE) modeling system and integration with Models-3. *The Emission Inventory: Regional Strategies for the Future*, *1461*.

Kinosian, J. R. (1982), Ozone precursor relationships from EKMA diagrams. *Environ. Sci. Technol.* 16, no. 12: 880-883.

Koo, B., N. Kumar, E. Knipping, U. Nopmongcol, T. Sakulyanontvittaya, M. T. Odman, A. G. Russell, and G. Yarwood (2015), Chemical transport model consistency in

475 simulating regulatory outcomes and the relationship to model performance. *Atmos.*
476 *Environ., 116*, 159–171.
477 Kota, S. H., G. Schade, M. Estes, D. Boyer, and Q. Ying (2015), Evaluation of MEGAN
478 predicted biogenic isoprene emissions at urban locations in Southeast Texas. *Atmos.*
479 *Environ.* 110, 54-64.
480 Loughner, C. P., D. J. Allen, K. E. Pickering, D. L. Zhang, Y. X. Shou, and R. R.
481 Dickerson (2011), Impact of fair-weather cumulus clouds and the Chesapeake Bay
482 breeze on pollutant transport and transformation. *Atmos. Environ., 45(24)*, 4060–4072.
483 Mao, J., F. Paulot, D. J. Jacob, R. C. Cohen, J. D. Crounse, P. O. Wennberg, C. A. Keller,
484 R. C. Hudman, M. P. Barkley, and L. W. Horowitz (2013), Ozone and organic nitrates
485 over the eastern United States: Sensitivity to isoprene chemistry. *J. Geophys. Res.-*
486 *Atmos., 118(19),* 11,256–11,268.
487 Martins, D. K., R. M. Stauffer, A. M. Thompson, T. N. Knepp, and M. Pippin (2012),
488 Surface ozone at a coastal suburban site in 2009 and 2010: relationships to chemical
489 and meteorological rocesses. *Journal of Geophys. Res.-Atmos. 117*(D5), D05306.
490 Perring, A. E., S. E. Pusede, and R. C. Cohen (2013), An observational perspective on the
491 atmospheric impacts of alkyl and multifunctional nitrates on ozone and secondary
492 organic aerosol. *Chemical Reviews, 113*, 5848 – 5870.
493 Pouliot, G., and T. E. Pierce (2009), *Integration of the Model of Emissions of Gases and*
494 *Aerosols from Nature (MEGAN) into the CMAQ Modeling System*. Retrieved from
495 http://www3.epa.gov/ttnchie1/conference/ei18/session3/pouliot.pdf
496 Ramboll Environ. (2014). *CAMx Version 6.10 User's Guide*. Retrieved November 2015
497 from http://www.camx.com/files/camxusersguide_v6-10.pdf
498 Sillman, S. (1999), The relation between ozone, NOx and hydrocarbons in urban and
499 polluted rural environments. *Atmos. Environ.*, *33*(12), 1821-1846.
500 Simon, H., K. R. Baker, and S. Phillips (2012) Compilation and interpretation of
501 photochemical model performance statistics published between 2006 and 2012. *Atmos.*
502 *Environ.* 61, 124-139.
503 Skamarock, W. C., J. B. Klemp, J. Dudhia, D. O. Gill, D. M. Barker, W. Wang, and J. G.
504 Powers. 2008, A description of the advanced WRF version 3. *NCAR technical note*
505 *NCAR/TN/u2013475+ STR*.
506 Thompson, A. M., R. M. Stauffer, S. K. Miller, D. K. Martins, E. Joseph, A. J.
507 Weinheimer, and G. S. Diskin (2014), Ozone profiles in the Baltimore-Washington
508 region (2006 – 2011): satellite comparisons and DISCOVER-AQ observations. *J.*
509 *Atmos. Chem.* 1-30.
510 Warneke, C., J. A. de Gouw, L. Del Negro, J. Brioude, S. McKeen, H. Stark, W. C.
511 Kuster, P. D. Goldan, M. Trainer, F. C. Fehsenfeld, C. Wiedinmyer, A. B. Guenther, A.
512 Hansel, A. Wisthaler, E. Atlas, J. S. Holloway, T. B. Ryerson, J. Peischl, L. G. Huey,
513 and A. T. Case Hanks (2010), Biogenic emission measurement and inventories
514 determination of biogenic emissions in the eastern United States and Texas and
515 comparison with biogenic emission inventories. *J. Geophys. Res.-Atmos.* 115, D00F18
516 Williams, E. J., K. Baumann, J. M. Roberts, S. B. Bertman, R. B. Norton, F. C.
517 Fehsenfeld, S. R. Springston, L. J. Nunnermacker, L. Newman, and K. Olszyna (1998)
518 Intercomparison of ground based NOy measurement techniques. *Journal of Geophys.*
519 *Res.-Atmos., 103*(D17), 22261–22280.

520 Yarwood, G, S. Rao, M. Yocke, and G. Whitten (2005), Updates to the Carbon Bond
521 chemical mechanism: CB05. *Final report to the US EPA, RT-0400675*, *8*.
522 Yu, S., R. Mathur, J. Pleim, G. Pouliot, D. Wong, B. Eder, K. Schere, R. Gilliam, and ST
523 Rao. 2012. Comparative evaluation of the impact of WRF/NMM and WRF/ARW
524 meteorology on CMAQ simulations for PM2. 5 and its related precursors during the
525 2006 TexAQS/GoMACCS study. *Atmos. Chem. Phys* 12, 4091-4106.
526 Zhou, W., D. S. Cohan, and S. L. Napelenok. 2013. Reconciling NO_x emissions
527 reductions and ozone trends in the US, 2002-2006. *Atmos. Environ.* 70, 236-244.
528

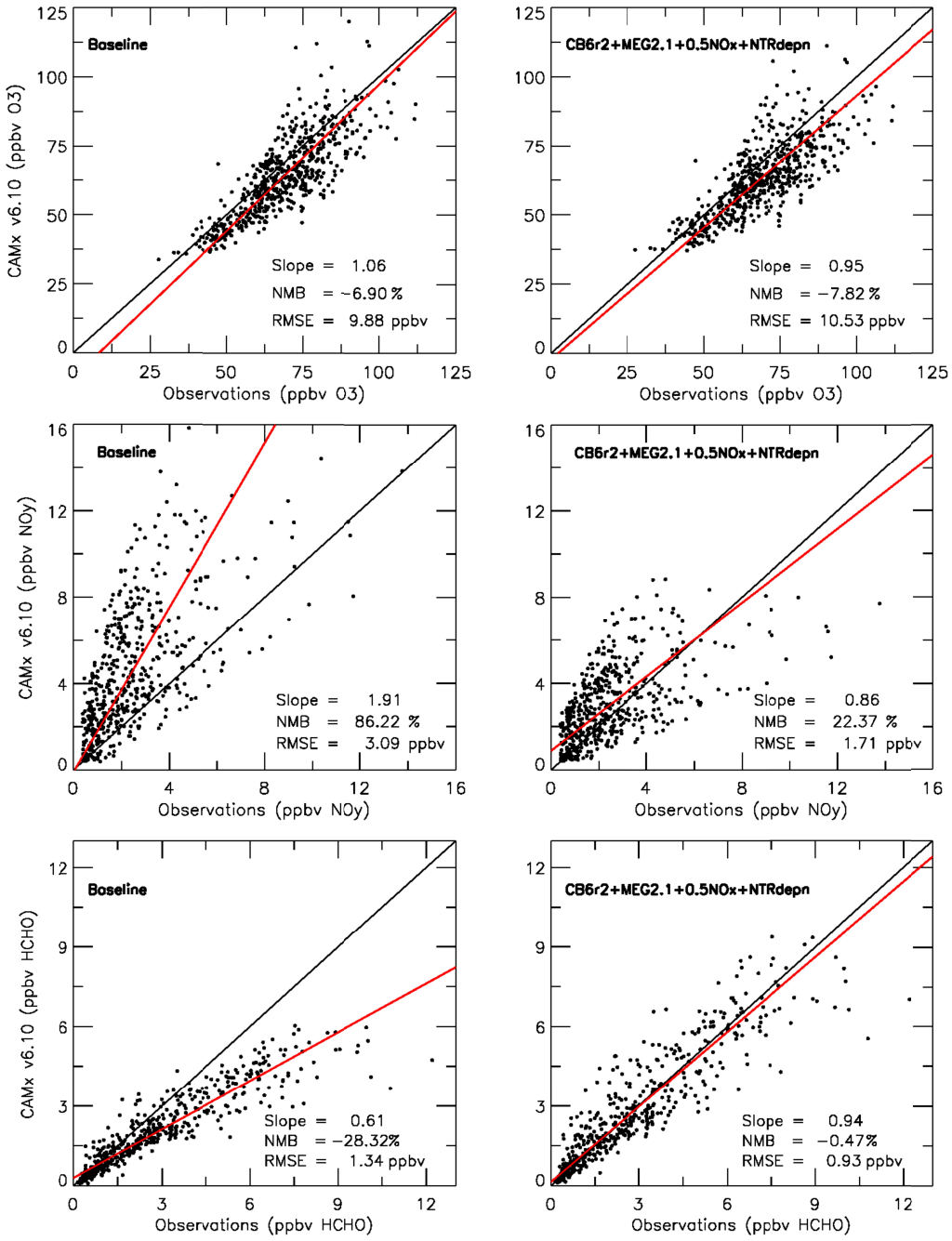

530

538 Figure 1. Observations acquired by the P3-B aircraft during DISCOVER-AQ Maryland
539 in July 2011 compared to model output from CAMx v6.10 at the nearest model grid point
540 and closest hourly interval. The closest hourly model output is matched to each one-
541 minute averaged P3-B observation; both quantities are then averaged over the same ten-
542 minute interval. Left panels show the baseline simulation, while right panels show the
543 updated "Beta" simulation. Top row shows O_3, middle row shows NO_y, and bottom row
544 shows HCHO. Black lines represent the 1:1 line, while red lines represent the linear best
545 fit.

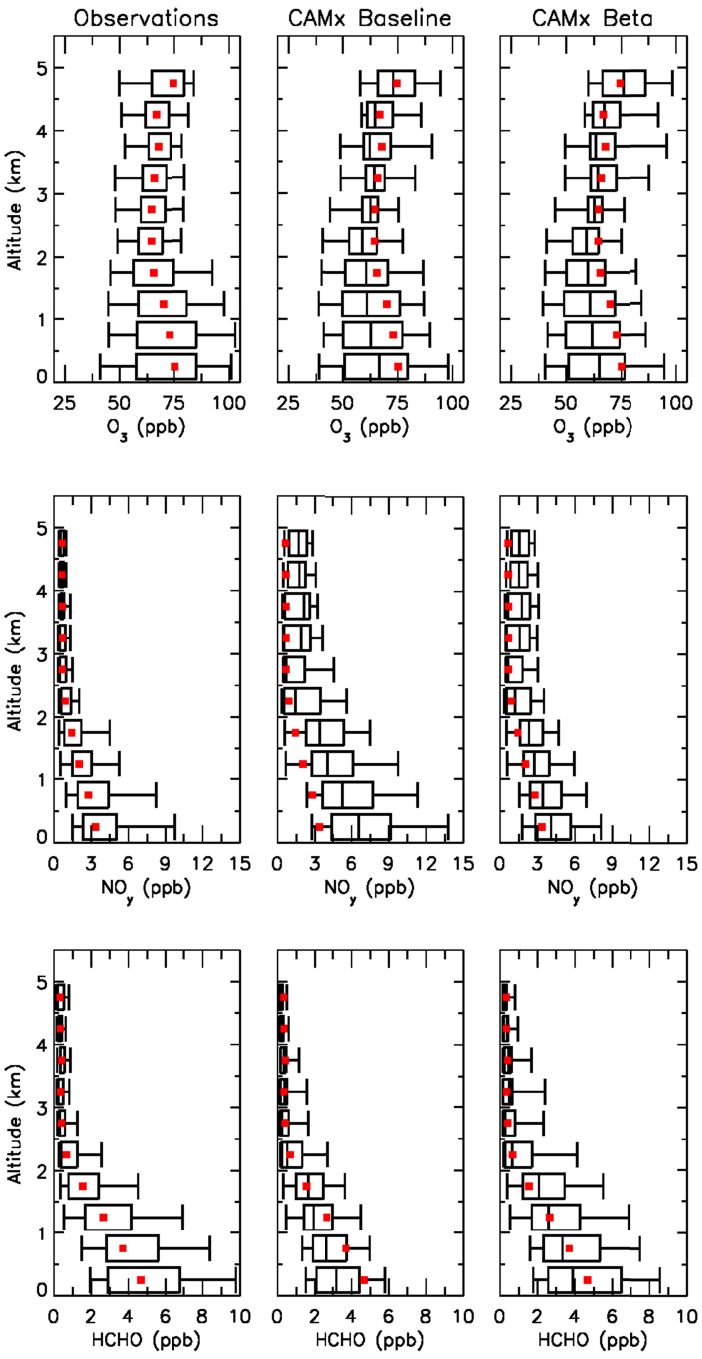

Figure 2. Vertical profiles of O_3, NO_y, and HCHO binned in 500 m intervals, showing the 5th, 25th, 50th, 75th and 95th percentiles. Left panels show one-minute averaged data from the P3-B aircraft, center panels show the baseline simulation, and the right panels show the updated "Beta" simulation. Model output from CAMx v6.10 is matched spatially and temporally to the P3-B measurements at one-minute intervals. Top row shows O_3, middle row shows NO_y, and bottom row shows HCHO. Red squares indicate the median values of the observations, which are shown on all panels to facilitate visual comparison.

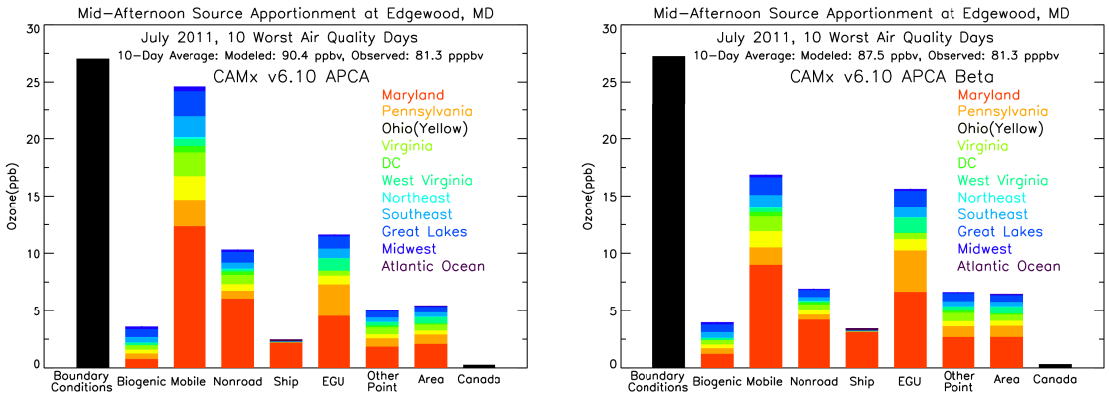

Figure 3. Ozone attributed to source sectors separated by U.S. states and the region of Canada that is in the modeling domain (Figure S1) during the ten worst air quality days in July 2011 at 2 PM local time at the Edgewood, MD monitoring site, located 30 km east-northeast of Baltimore: (left) baseline simulation and (right) updated "Beta" simulation.

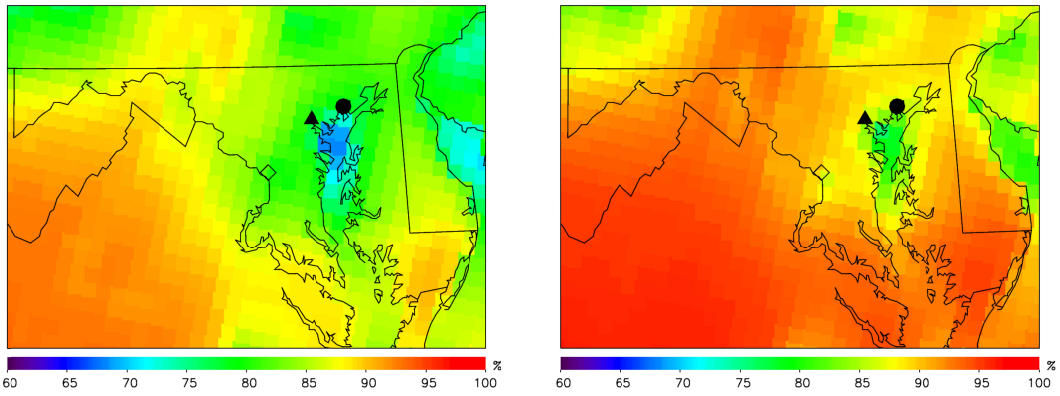

Figure 4. Percentage of ozone formed in the NO_x–limited production regime during July 2011 averaged over daytime (8 AM – 8 PM local time) for the entire month in the (left) baseline simulation and (right) updated "Beta" simulation. The filled triangle denotes Baltimore, Maryland and the filled circle denotes Edgewood, Maryland.

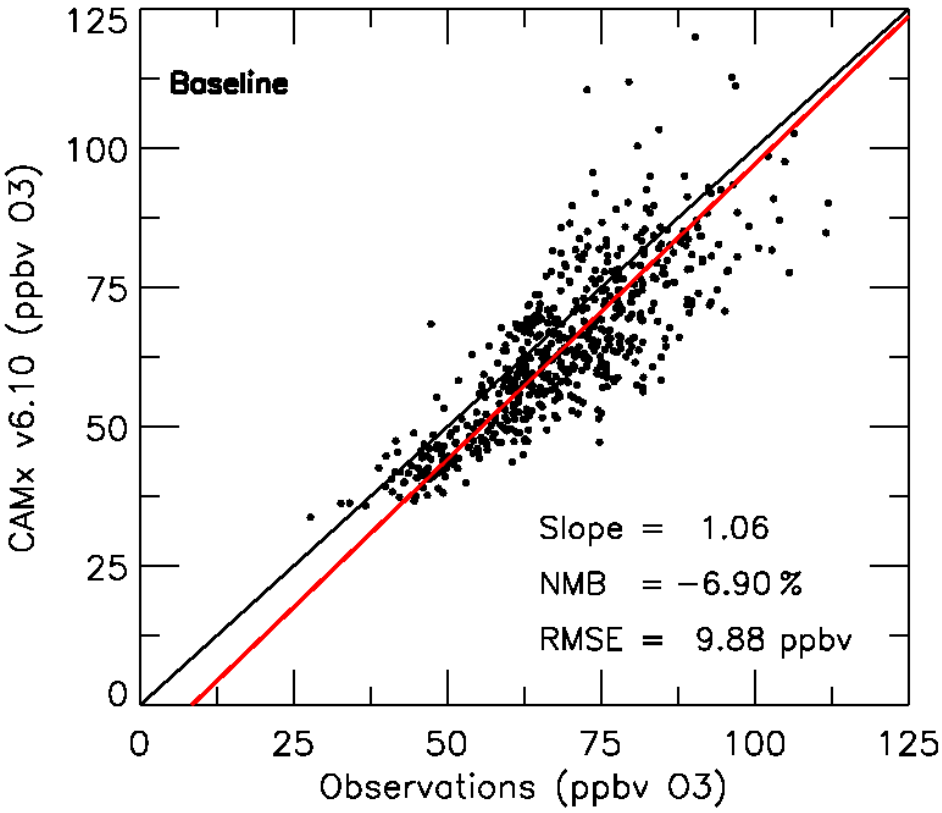
Baseline
Slope = 1.06
NMB = −6.90 %
RMSE = 9.88 ppbv
CAMx v6.10 (ppbv O3)
Observations (ppbv O3)
0
25
50
75
100
125

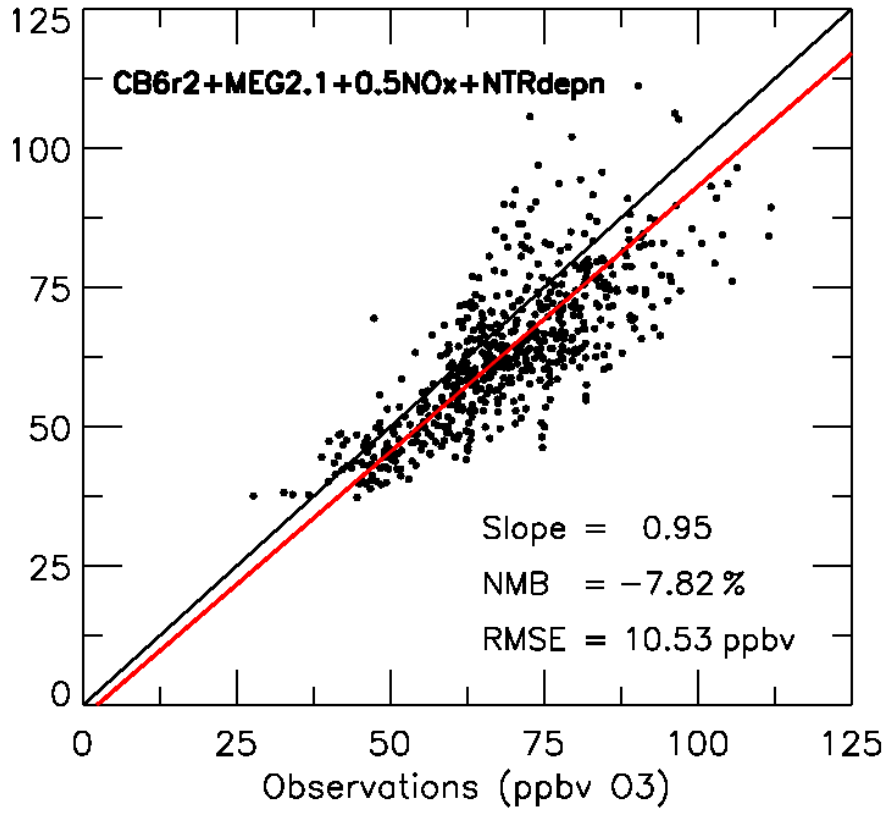
CB6r2+MEG2.1+0.5NOx+NTRdepn
Slope = 0.95
NMB = −7.82 %
RMSE = 10.53 ppbv
Observations (ppbv O3)
0
25
50
75
100
125

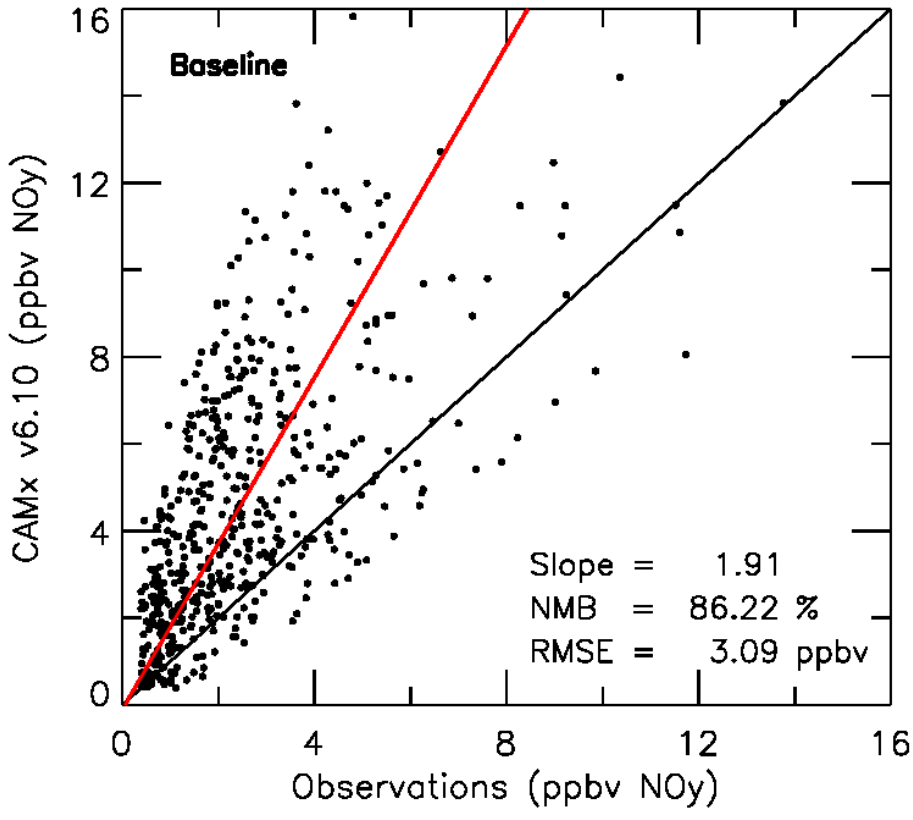
Baseline
Slope = 1.91
NMB = 86.22 %
RMSE = 3.09 ppbv
CAMx v6.10 (ppbv NOy)
Observations (ppbv NOy)
0
4
8
12
16

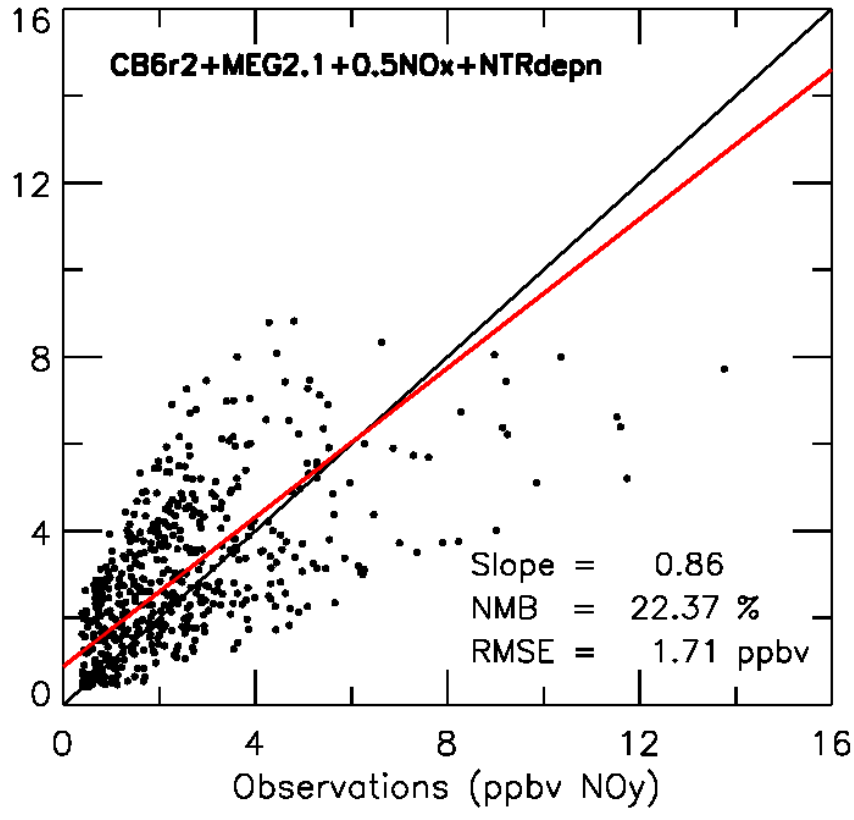
CB6r2+MEG2.1+0.5NOx+NTRdepn
Slope = 0.86
NMB = 22.37 %
RMSE = 1.71 ppbv
Observations (ppbv NOy)
0
4
8
12
16

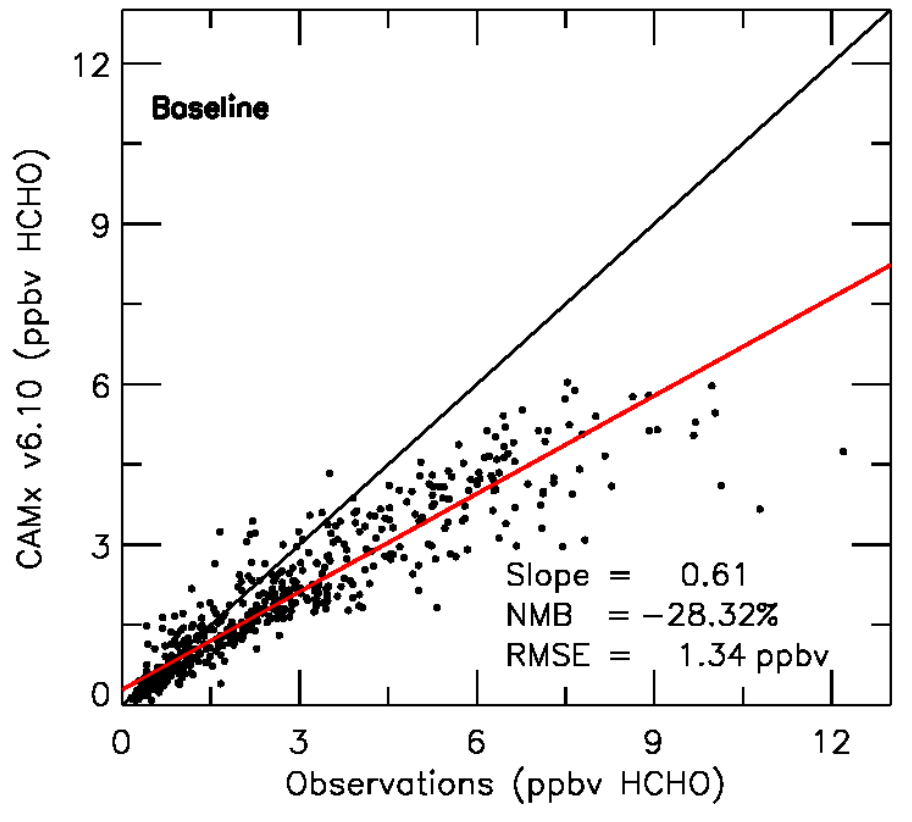
Baseline
Slope = 0.61
NMB = −28.32%
RMSE = 1.34 ppbv
CAMx v6.10 (ppbv HCHO)
Observations (ppbv HCHO)
0
3
6
9
12

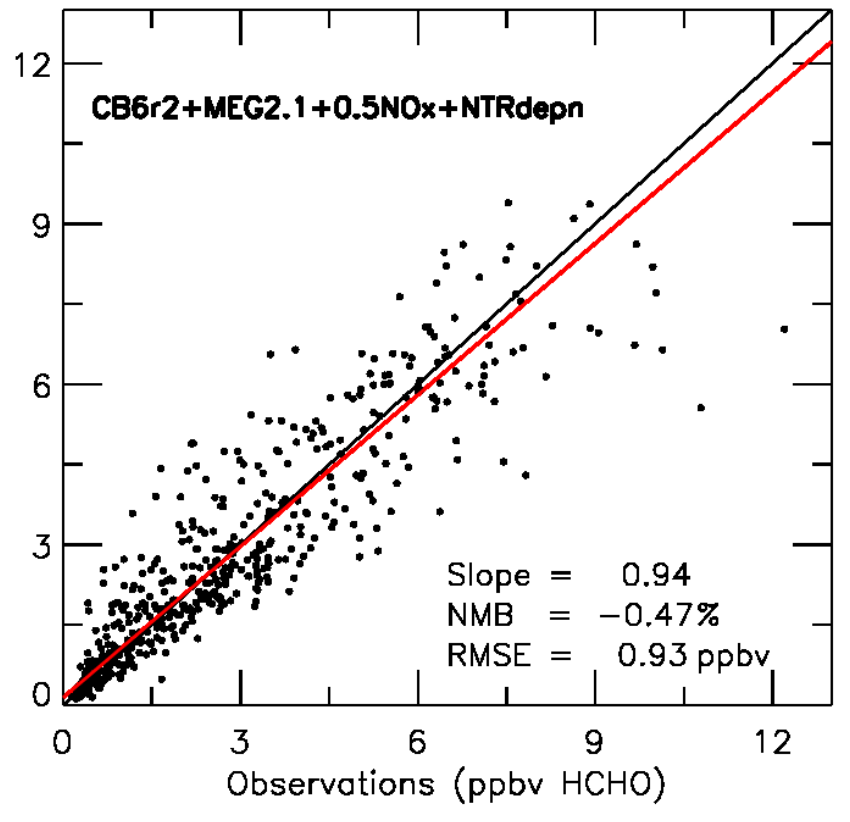
CB6r2+MEG2.1+0.5NOx+NTRdepn
Slope = 0.94
NMB = −0.47%
RMSE = 0.93 ppbv
Observations (ppbv HCHO)
0
3
6
9
12

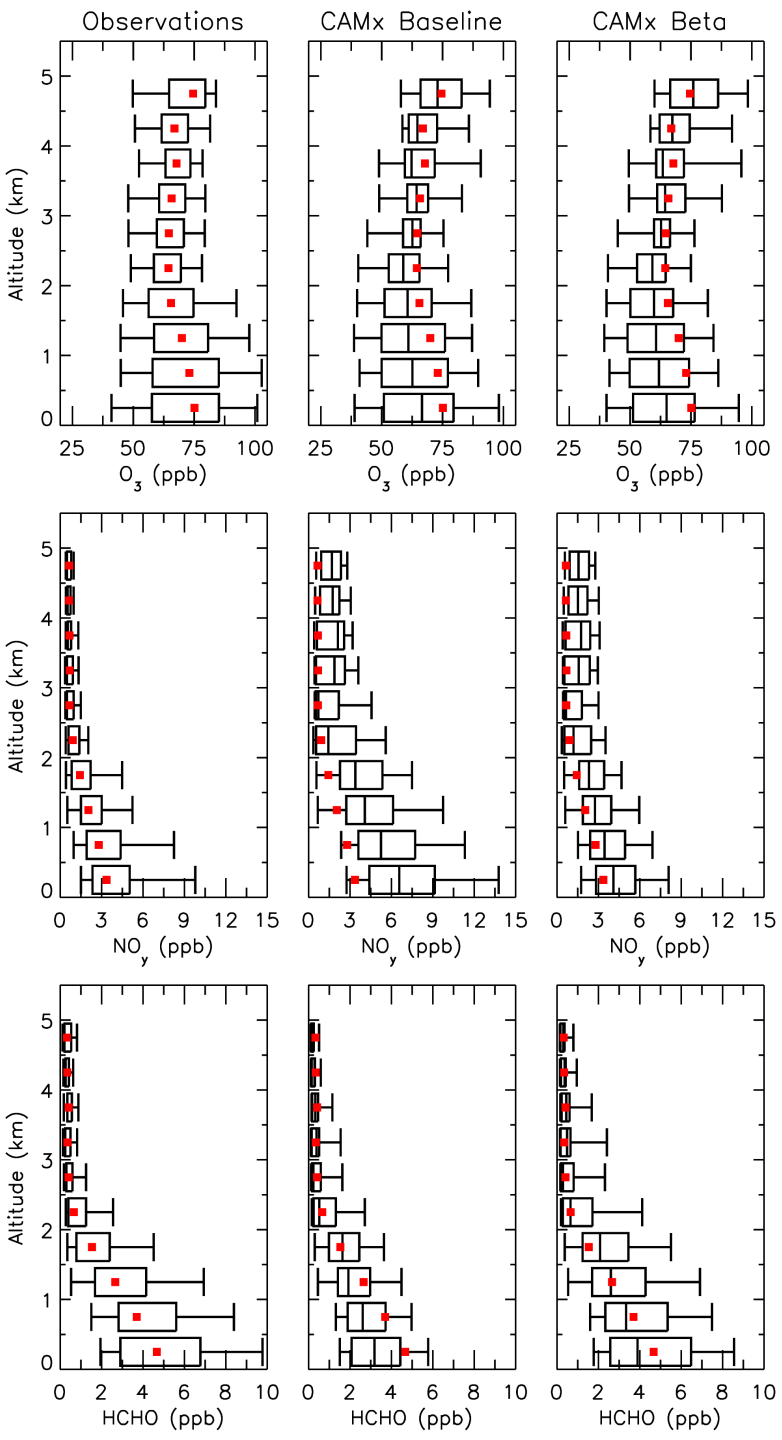
Observations
CAMx Baseline
CAMx Beta
Altitude (km)
0
1
2
3
4
5
25
50
75
100
O_3 (ppb)
0
3
6
9
12
15
NO_y (ppb)
0
2
4
6
8
10
HCHO (ppb)

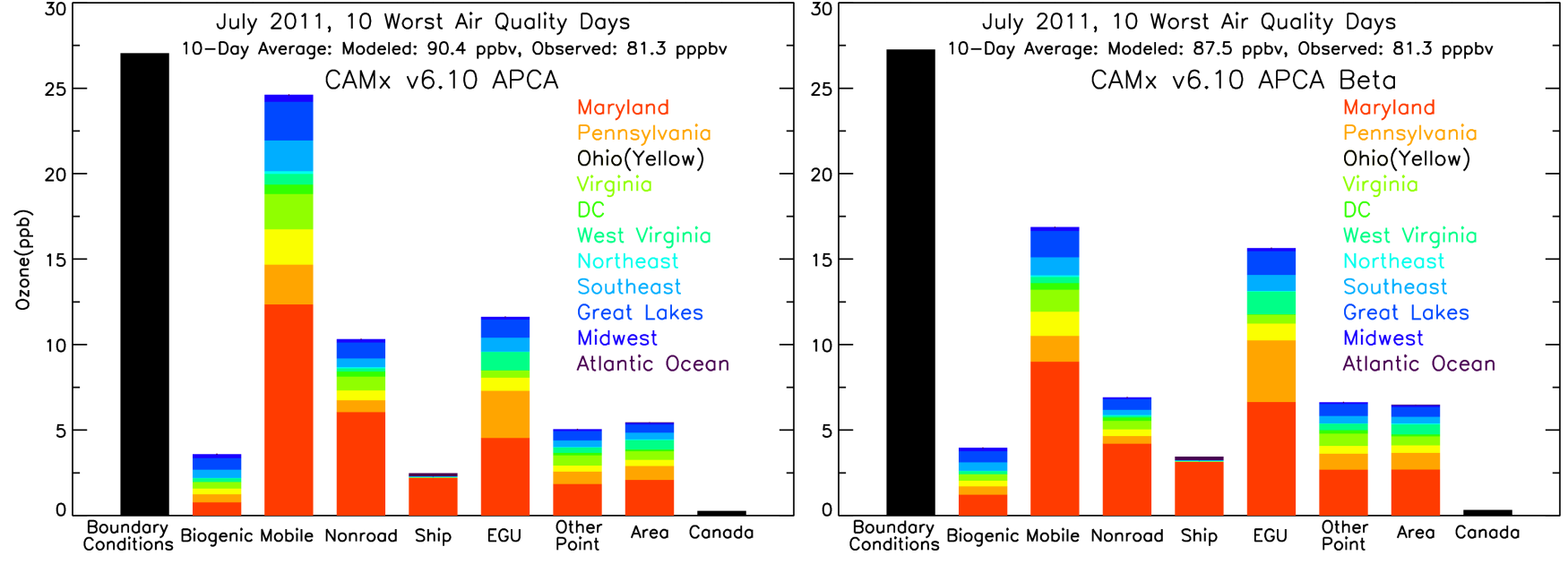
July 2011, 10 Worst Air Quality Days
10-Day Average: Modeled: 90.4 ppbv, Observed: 81.3 pppbv
CAMx v6.10 APCA
Ozone(ppb)
Maryland
Pennsylvania
Ohio(Yellow)
Virginia
DC
West Virginia
Northeast
Southeast
Great Lakes
Midwest
Atlantic Ocean
Boundary Conditions
Biogenic
Mobile
Nonroad
Ship
EGU
Other Point
Area
Canada
July 2011, 10 Worst Air Quality Days
10-Day Average: Modeled: 87.5 ppbv, Observed: 81.3 pppbv
CAMx v6.10 APCA Beta

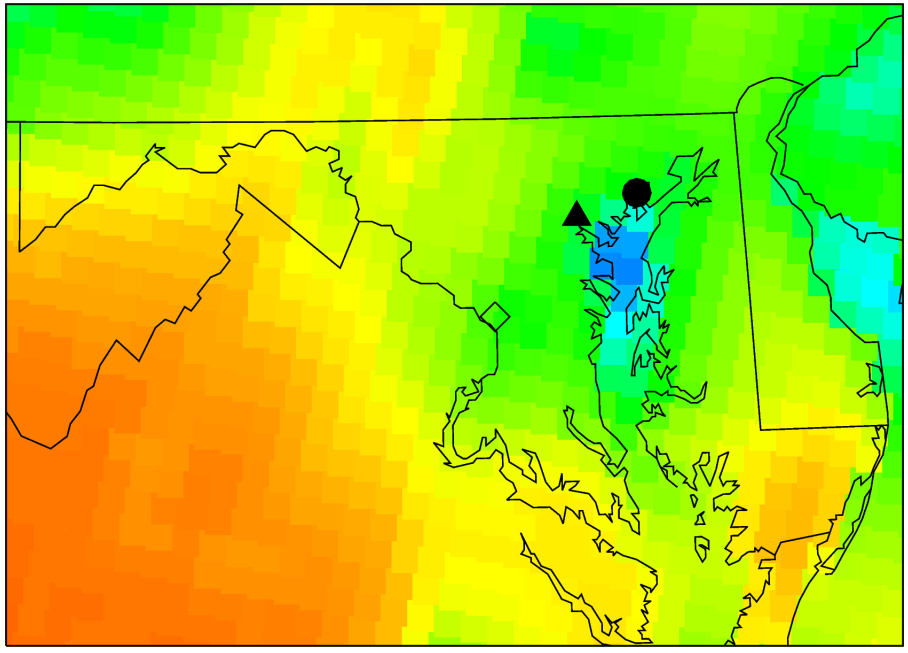

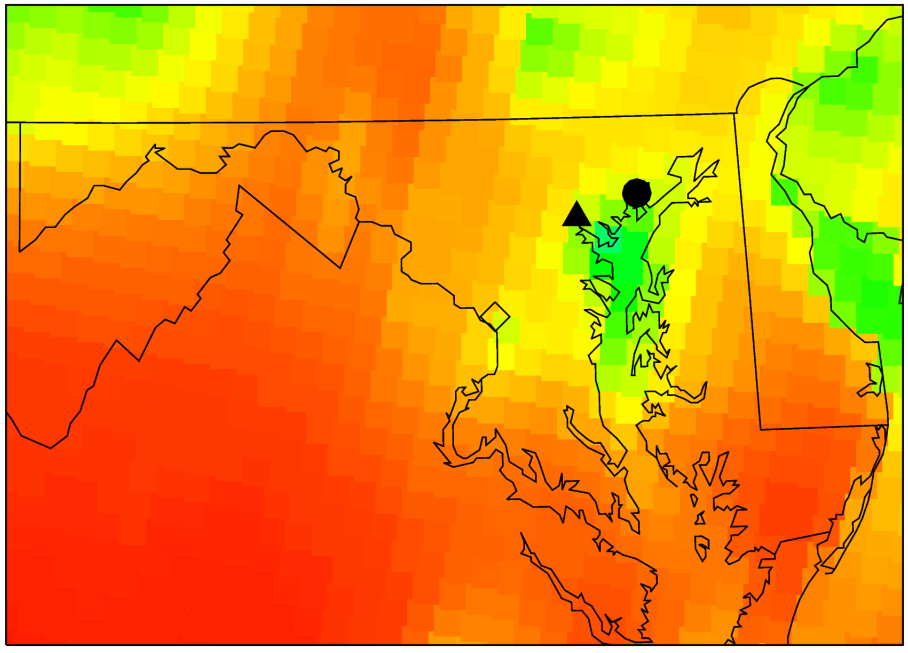

60 65 70 75 80 85 90 95 100 %

60 65 70 75 80 85 90 95 100 %